

## Rapid Synthesis and Charge–Discharge Properties of LiMnPO<sub>4</sub> Nanocrystallite-embedded Porous Carbons

Shintaro Aono,<sup>1</sup> Koki Urita,<sup>2</sup> Hirotochi Yamada,<sup>2</sup> and Isamu Moriguchi\*<sup>2</sup>

<sup>1</sup>Graduate School of Science and Technology, 1-14 Bunkyo-machi, Nagasaki 852-8521

<sup>2</sup>Graduate School of Engineering, Nagasaki University, 1-14 Bunkyo-machi, Nagasaki 852-8521

(Received November 21, 2011; CL-111123; E-mail: mrgch@nagasaki-u.ac.jp)

LiMnPO<sub>4</sub> nanocrystallite-embedded porous carbons were successfully synthesized within a few minutes by a microwave-heating process. The nanocomposites showed higher charge–discharge capacity and better rate capability than bulk-LiMnPO<sub>4</sub> particles synthesized in a similar manner without porous carbons.

Olivine-type lithium metal phosphates have attracted much attention as a potential cathode material for secondary lithium-ion batteries due to the relatively high theoretical capacity (ca. 170 mA h g<sup>-1</sup>) as well as thermal and electrochemical stabilities. However, these materials have intrinsically poor electronic conductivity and Li-ion diffusivity, and hence poor rate capability.<sup>1</sup> Down sizing Li host particles is effective to overcome the latent problem of LiFePO<sub>4</sub><sup>2,3</sup> but not enough for LiMnPO<sub>4</sub> having much lower conductivity of than LiFePO<sub>4</sub>.<sup>4,5</sup> It was reported that the poor rate capability of LiMnPO<sub>4</sub> is ascribable to a large kinetic barrier at the mismatched interface of MnPO<sub>4</sub>/LiMnPO<sub>4</sub> during Li insertion/extraction processes and that down sizing the olivine particle to nanometer level would be effective to lower the kinetic barrier.<sup>6</sup> Since LiMnPO<sub>4</sub> is expected to have higher energy density than LiFePO<sub>4</sub> due to its higher redox potential of 4.1 V vs. Li/Li<sup>+</sup> (3.5 V vs. Li/Li<sup>+</sup> for LiFePO<sub>4</sub>), various methods to synthesize nanosized LiMnPO<sub>4</sub> particles have been developed in recent years for achieving reasonable capacity and rate. However, there is still a problem of poor electronic conductivity in the electrode because strong agglomeration of nanosized particles prevents homogeneous mixing with a conductive additive such as carbon black.

The present study shows the first attempt for synthesis of LiMnPO<sub>4</sub> nanocrystallites in the nanopores or on the pore walls of nanoporous carbons. Here the nanoporous carbon provides electron-conduction and ion-transport paths in the composite. Indeed it has been recently reported that nanoporous composites of TiO<sub>2</sub>/CNTs and V<sub>2</sub>O<sub>5</sub>/porous carbon exhibited excellent rate of Li insertion/extraction.<sup>7–9</sup> Therefore, the present composite is expected to facilitate electrochemical reactions of LiMnPO<sub>4</sub> nanocrystallites. In addition, the present study succeeded in a rapid synthesis of LiMnPO<sub>4</sub> nanocrystallites within a few minutes through a local heating of carbon framework using a microwave irradiation, contrasting the reported synthetic processes such as a conventional solid-state,<sup>1</sup> sol–gel,<sup>5</sup> and polyol<sup>10</sup> methods requiring several hours to produce LiMnPO<sub>4</sub> crystals. Although colloidal crystal-derived porous carbons were employed here as a representative carbon framework, the present methodology is applicable in principle to various porous carbons such as activated carbons which can be easily obtained.

Nanoporous carbons with an average pore diameter of 110 or 450 nm were obtained by a SiO<sub>2</sub>-opal template process

as previously reported.<sup>11,12</sup> An inorganic source solution for LiMnPO<sub>4</sub> synthesis was prepared by dissolving LiH<sub>2</sub>PO<sub>4</sub> and Mn(CH<sub>3</sub>COO)<sub>2</sub>·4H<sub>2</sub>O in diethylene glycol with the molar ratio of Li/Mn/P = 1/1/1, in which a small amount of nitric acid was added to yield a clear solution. 0.2 g of the nanoporous carbon was dispersed in 20 mL of the inorganic source solution, then the solution was subjected to microwave irradiation (2.45 GHz, 400 W) for several minutes. The precipitated product was filtered off, washed with deionized water and acetone, and dried at 110 °C in air for 12 h. The porous carbons and composite samples are denoted as PC<sub>x</sub> and LMP–PC<sub>x</sub>[*T-t*], where *x*, *T*, and *t* are the average pore diameter of porous carbon, microwave irradiation temperature (200 or 250 °C), and the irradiation time (5 or 8 min). As a reference, bulk LiMnPO<sub>4</sub>, LMP[*T-t*], was also synthesized without the porous carbon in a similar manner.

Figure 1 shows XRD patterns of the samples obtained in this study. All the XRD peaks were assigned to an olivine-type LiMnPO<sub>4</sub> with orthorhombic *Pnma* space group. The intensity of (020) peak was higher than that of (311) in all the samples in contrast to the standard XRD pattern (PDF: 01-072-7844). *b*-Axis oriented crystallites were produced in the present synthesis, similar to the reported method of refluxing a diethylene glycol solution dissolved inorganic source,<sup>10</sup> but the product was obtained within a few minutes in the present synthesis. As can be seen in Figure 2a, LMP[200-8], which was obtained without porous carbons, was flake-like particles with the 2D-plane size of several micrometers, suggesting anisotropic crystal growth. On the other hand, LMP–PC composite samples possessed nanoporous morphology based on porous carbons where most of LMP nanocrystallites were deposited in the nanopores and some of them were on the outersurface (Figure 2b). The size of observed LMP nanocrystallites was 20–30 nm, which was

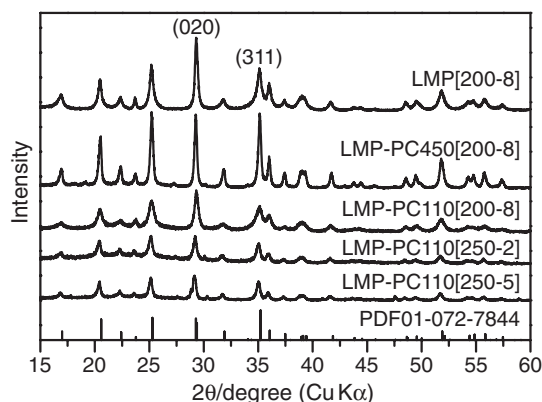
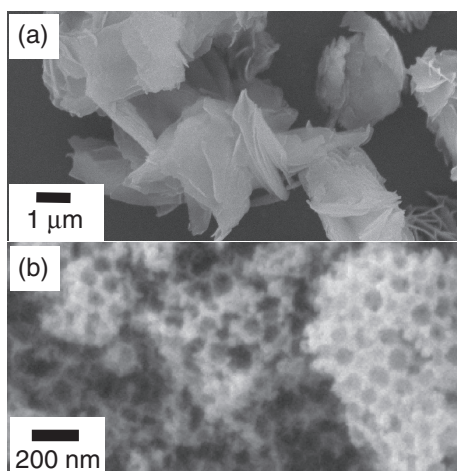


Figure 1. XRD patterns of the samples.



**Figure 2.** SEM images of (a) LMP[200-8] and (b) LMP-PC110[250-5].

**Table 1.** Specific surface area ( $S_a$ ) and carbon content of samples

Samples	$S_a/\text{m}^2\text{g}^{-1}$ (micropore $S_a$ , macropore $S_a$ ) <sup>b</sup>	C content /wt %
PC450	1236 (1080, 156)	100
PC110	1263 (796, 467)	100
LMP[200-8]	64 (—, —)	n.d. <sup>c</sup>
LMP-PC450[200-8]	151 (161, 329)	30.9
LMP-PC110[200-8]	300 (244, 488)	43.3
LMP-PC110[250-5]	344 (240, 411)	53.7

<sup>a</sup>Total surface area based on the composite weight. <sup>b</sup>Based on the carbon weight. <sup>c</sup>n.d.: not detected.

comparable to that estimated from the full width at half-maximum (FWHM) of XRD peaks by using the Scherrer equation.<sup>13</sup> The large flakes of LMP[200-8] were little observed in LMP-PCx[*T*-*l*] samples. Specific surface area ( $S_a$ ) and carbon content of the samples are listed in Table 1. The  $S_a$  values were determined by the  $\alpha_s$ -plot analysis using the subtracting pore effect (SPE) from  $\text{N}_2$  adsorption isotherms,<sup>11</sup> and the carbon content was analyzed by thermogravimetric measurements in air. Although LMP-PCx[200-8] samples had higher  $S_a$  values than LMP[200-8], the  $S_a$  values of LMP-PCx[200-8] samples were quite smaller than the weighted average values ( $S_{a,w}$ ) calculated under the assumption of a simple mixing of LMP[200-8] and PC110;  $S_{a,w}$  values of LMP-PC110[200-8] and LMP-PC450[200-8] were 530 and 360  $\text{m}^2\text{g}^{-1}$ , respectively. This means that LMP nanocrystallites were produced preferentially in nanopores of porous carbons. Moreover, the LMP deposition made the micropore surface area based on carbon weight decreased largely while keeping the macropore surface area almost the same as that of the pristine porous carbon, indicating that the LMP nanocrystallites were deposited on the surface of macropore carbon wall to cover micropores existed in the wall. It can be concluded from these results that LMP nanocrystallite-embedded porous carbons were successfully synthesized in the present process.

Electrochemical charge–discharge measurements were carried out in a 1.0  $\text{mol dm}^{-3}$  solution of  $\text{LiPF}_6$  in ethylene

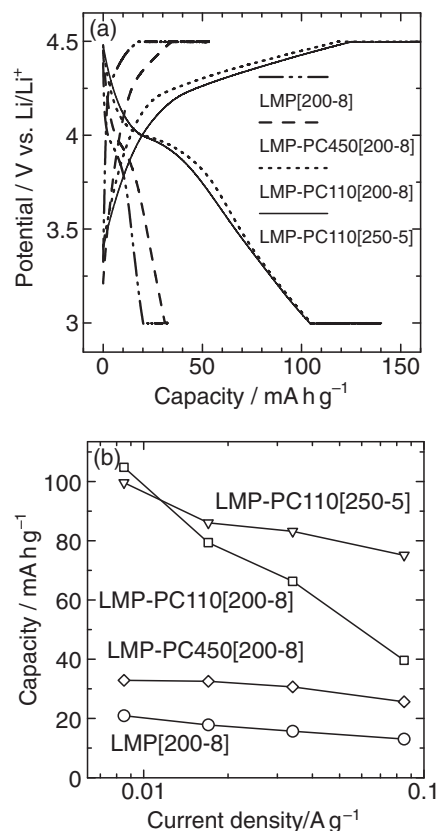


**Figure 3.** Charge–discharge property of samples; (a) initial charge–discharge curves and (b) rate capability.

carbonate/dimethyl carbonate (1/1 by volume) using a sealed three-electrode beaker cell or a CR2032 coin cell equipped Li counter and reference electrodes. The LMP-PC composites mixed with poly(tetrafluoroethylene), the weight ratio of which was 90/10, were pressed onto an Al mesh and then were used as the working electrodes. For the LMP[200-8] which had no carbon content, 40 wt % acetylene black was also mixed in the preparation of working electrode. Charge–discharge curves were obtained by a constant current (CC)–subsequent constant voltage (CV) mode at the voltage range of 3.0–4.5 V vs.  $\text{Li/Li}^+$  at room temperature. Figure 3a shows initial charge–discharge curves of samples at 0.05 C ( $1\text{ C} = 171\text{ mA g}^{-1}$ ). All the samples exhibited a plateau around 4.0 V vs.  $\text{Li/Li}^+$  in discharge curves, which is characteristic of  $\text{LiMnPO}_4$ . The LMP-PC composite samples possessed higher capacity than LMP[200-8], and further increase in capacity was observed on the nanocomposites of a porous carbon with smaller pore size (PC110). The LMP-PC110 samples showed higher capacities even at high current densities as shown in Figure 3b. However, the capacity of composite samples at low C rates such as 0.1 C was not so high in comparison with that in recent reports,<sup>5,10,14–18</sup> suggesting that some of LMP crystallites, produced outside of carbon nanopores, might not contribute to the charging–discharging due to insufficient electronic supply. On the other hand, the composite samples possessed a high rate capability; LMP-PC110[250-5] showed a capacity retention of 87% at 0.5 C against 0.1 C, which was comparable to or higher than that reported.<sup>5,10,14–18</sup> It was also confirmed that the composite samples showed stable cycle

performance except for an initial few cycles (Figure S1 in Supporting Information<sup>19</sup>). These results mean that LMP nanocrystallites successfully embedded in the nanoporous carbon possess high charging–discharging performance. The three-dimensionally continuous carbon framework and nanosized crystallites would suppress polarization during charging–discharging.

In conclusion, we succeeded in a rapid synthesis of LiMnPO<sub>4</sub> nanocrystallites in nanoporous carbons by using a microwave-heating process. The nanocomposite structure was effective to improve the charge–discharge property of LiMnPO<sub>4</sub>. Further study on the optimization of nanocomposite structure by controlling pore size, crystallite size, and LiMnPO<sub>4</sub> loading amount will bring out better performance of LiMnPO<sub>4</sub> although the capacity of present materials is still lower than the theoretical value.

This study made use of XRD in the Center for Instruments Analysis of Nagasaki University. This work was partly supported by a Grant-in-Aid for Scientific Research from the Ministry of Education, Culture, Sports, Science and Technologies of Japan.

#### References and Notes

- 1 C. Delacourt, L. Laffont, R. Bouchet, C. Wurm, J.-B. Leriche, M. Morcrette, J.-M. Tarascon, C. Masquelier, *J. Electrochem. Soc.* **2005**, *152*, A913.
- 2 D.-H. Kim, J. Kim, *Electrochem. Solid-State Lett.* **2006**, *9*, A439.
- 3 B. Kang, G. Ceder, *Nature* **2009**, *458*, 190.
- 4 T. Drezzen, N.-H. Kwon, P. Bowen, I. Teerlinck, M. Isono, I. Exnar, *J. Power Sources* **2007**, *174*, 949.
- 5 C. Delacourt, P. Poizot, M. Morcrette, J.-M. Tarascon, C. Masquelier, *Chem. Mater.* **2004**, *16*, 93.
- 6 M. Yonemura, A. Yamada, Y. Takei, N. Sonoyama, R. Kanno, *J. Electrochem. Soc.* **2004**, *151*, A1352.
- 7 I. Moriguchi, R. Hidaka, H. Yamada, T. Kudo, H. Murakami, N. Nakashima, *Adv. Mater.* **2006**, *18*, 69.
- 8 I. Moriguchi, Y. Shono, H. Yamada, T. Kudo, *J. Phys. Chem. B* **2008**, *112*, 14560.
- 9 H. Yamada, K. Tagawa, M. Komatsu, I. Moriguchi, T. Kudo, *J. Phys. Chem. C* **2007**, *111*, 8397.
- 10 D. Wang, H. Buqa, M. Crouzet, G. Deghenghi, T. Drezzen, I. Exnar, N.-H. Kwon, J. H. Miners, L. Poletto, M. Grätzel, *J. Power Sources* **2009**, *189*, 624.
- 11 I. Moriguchi, F. Nakahara, H. Furukawa, H. Yamada, T. Kudo, *Electrochem. Solid-State Lett.* **2004**, *7*, A221.
- 12 H. Yamada, H. Nakamura, F. Nakahara, I. Moriguchi, T. Kudo, *J. Phys. Chem. C* **2007**, *111*, 227.
- 13 B. D. Cullity, *Elements of X-ray Diffraction*, Addison-Wesley, Reading, MA, **1956**.
- 14 D. Choi, D. Wang, I.-T. Bae, J. Xiao, Z. Nie, W. Wang, V. V. Viswanathan, Y. J. Lee, J.-G. Zhang, G. L. Graff, Z. Yang, J. Liu, *Nano Lett.* **2010**, *10*, 2799.
- 15 S.-M. Oh, S.-W. Oh, C.-S. Yoon, B. Scrosati, K. Amine, Y.-K. Sun, *Adv. Funct. Mater.* **2010**, *20*, 3260.
- 16 Z. Bakenov, I. Taniguchi, *J. Power Sources* **2010**, *195*, 7445.
- 17 J. Ni, Y. Kawabe, M. Morishita, M. Watada, T. Sakai, *J. Power Sources* **2011**, *196*, 8104.
- 18 F. Wang, J. Yang, P. Gao, Y. NuLi, J. Wang, *J. Power Sources* **2011**, *196*, 10258.
- 19 Supporting Information is available electronically on the CSJ-Journal Web site, <http://www.csj.jp/journals/chem-lett/index.html>.